BIOENERGY AND BIOFUELS

A multi-electrode continuous flow microbial fuel cell with separator electrode assembly design

Yongtae Ahn · Bruce E. Logan

Abstract Scaling up microbial fuel cells (MFCs) requires the development of compact reactors with multiple electrodes. A scalable single chamber MFC (130 mL), with multiple graphite fiber brush anodes and a single air-cathode cathode chamber ($27 \ m^2/m^3$), was designed with a separator electrode assembly (SEA) to minimize electrode spacing. The maximum voltage produced in fed-batch operation was 0.65 V (1,000 Ω) with a textile separator, compared to only 0.18 V with a glass fiber separator due to short-circuiting by anode bristles through this separator with the cathode. The maximum power density was 975 mW/m^2, with an overall chemical oxygen demand (COD) removal of >90% and a maximum coulombic efficiency (CE) of 53% (50 Ω resistor). When the reactor was switched to continuous flow operation at a hydraulic retention time (HRT) of 8 h, the cell voltage was 0.21±0.04 V, with a very high CE=85%. Voltage was reduced to 0.13±0.03 V at a longer HRT=16 h due to a lower average COD concentration, and the CE (80%) decreased slightly with increased oxygen intrusion into the reactor per amount of COD removed. Total internal resistance was 33 Ω, with a solution resistance of 2 Ω. These results show that the SEA type MFC can produce stable power and a high CE, making it useful for future continuous flow treatment using actual wastewaters.

Keywords Microbial fuel cell · Scaling up · Separator electrode assembly · Continuous flow

Y. Ahn · B. E. Logan (✉)
Department of Civil & Environmental Engineering,
Penn State University,
212 Sackett Building,
University Park, PA 16802, USA
e-mail: blogan@psu.edu

Introduction

Microbial fuel cells (MFCs) are devices in which bacteria create electrical power by oxidizing simple compounds such as glucose or complex organic matter in wastewater (Logan 2008). Electrons released to the anode flow to cathode through an external circuit, with charge transferred through the solution (and membrane or spacer if present). Electrons and protons are consumed in the cathode, using an oxidizer such as oxygen (Logan et al. 2006; Logan 2008). Several types of MFCs have been developed in order to examine the effects of different architectures on performance, including two-chamber (Min and Logan 2004), single-chamber (Liu and Logan 2004), flat plate (Aelterman et al. 2006), and stacked reactors (Dekker et al. 2009). The main performance goals are increasing power densities, the recovery of electrons as current [coulombic efficiency (CE)], and energy recovery while using simple designs and low-cost materials (Logan et al. 2006). Improvement in MFC performance can be achieved by optimizing several factors including reducing the electrode spacing (Cheng et al. 2006b) while avoiding oxygen contamination of the anode, increased solution conductivity to reduce ohmic losses (Liu et al. 2005b), pre-acclimation of the inocula to optimize exoelectrogenic activity (Cheng and Logan 2011), and using low-cost electrode materials (Cheng and Logan 2007).

Scaling up MFCs requires compact reactor designs and the use of multiple electrodes. Several microbial electrolysis cells (MECs) have been designed with multiple anodes and cathodes (Rader and Logan 2010; Cusick et al. 2011), but there are few examples of MFCs with multiple electrodes (Liu et al. 2008; Dekker et al. 2009). Electrodes should be closely spaced to minimize ohmic losses (Liu et al. 2005a). However, this can decrease MFC performance due to oxygen crossover from the anode to the cathode, which reduces

power generation and CE due to aerobic respiration of bacteria (Cheng et al. 2006b). Ion exchange membranes can help reduce oxygen crossover and improve CEs, but they substantially reduce power production (Rozendal et al. 2007; Zhang et al. 2009, 2010a). An alternative to a using a membrane is to place a separator between the electrodes, allowing for more compact designs known as separator electrode assemblies (SEAs) (Zhang et al. 2011b). MFCs with SEAs can be used to generate higher power densities and higher CEs than systems with large electrode spacing (Pham et al. 2005; Zhang et al. 2010a, 2011b). Power densities as high as 1.55 kW/m^3 have been produced using very small (2.5 mL) air-cathode MFCs and SEAs with very large cathode-specific surface areas (280 m^2/m^3, cathode projected area per volume of reactor) (Fan et al. 2007). An even higher power density of 2.15 kW/m^3 was generated using an even smaller 0.335-mL MFC with a membrane and a ferricyanide solution, by using a disproportionately sized cathode surface area of 1,920 m^2/m^3 (16 times the area of the anode) (Nevin et al. 2008). The cathode limits power generation in most MFCs, and therefore, a large cathode-specific surface area can produce very high apparent power densities. However, the overall system is not scalable for practical applications unless air cathodes are used (to avoid the use of non-sustainable chemicals or aeration of water), and if the liquid volume is sufficient to avoid clogging. For example, very high media densities are known to result in clogging of trickling filters with biomass. Thus, the design of systems that have reasonable void volumes will be essential for wastewater treatment. In addition, SEA-type MFCs are likely essential for low conductivity wastewaters (~1 mS/cm) to avoid high ohmic losses. Even under optimal conditions of high solution conductivity and readily degradable substrates (such as acetate), maximum volumetric power of liter-scale MFCs have been less than 35 W/m^3 (Liu et al. 2008; Dekker et al. 2009). Thus, reactor performance with scaling is an important issue for harnessing power from wastewaters using MFCs.

In this study, MFCs with multiple anodes and SEAs were constructed and evaluated under both fed-batch and continuous flow operations. As reactor sizes increase and continuous flow conditions are used, the performance of the MFC with flow through the system will be critical for understanding useful performance conditions. Previous designs used in our laboratory, and by many others, have shown that brush anodes are beneficial for increasing power generation in MFCs (Logan et al. 2007; Feng et al. 2010; Hays et al. 2011). Brush anodes were used in a pilot-scale MFC study conducted by the University of Queensland, but performance results are not available, and only one anode was used per reactor (Logan 2010). Brush anodes were also used in a pilot-scale MEC, but not in conjunction with air cathodes (Cusick et al. 2011). Therefore, we constructed

multiple anode MFCs specifically to look at the effect of the flow over multiple anodes on performance in MFCs with air cathodes. While the reactor had a relatively modest liquid size (130 mL), the design used is inherently scalable. In order to benchmark the performance of this system against previous brush anode designs, power densities and electrical efficiencies were evaluated using buffered acetate solutions. Performance was examined under both fed-batch and continuous modes [at different hydraulic retention times (HRT) and external resistances] to better understand the effect of hydraulic flow through the reactor on performance. The internal resistance was measured and characterized in order to identify factors that could limit performance of these newly designed SEA type MFCs.

Materials and methods

MFC construction

A single-chamber, air cathode MFC was designed with an anode chamber volume of 130 mL (Fig. 1). Each reactor contained three anodes and a single cathode with 35 cm^2 exposed to air, producing a cathode-specific surface area of 27 m^2/m^3. Brush anodes (25-mm diameter by 35-mm length) were made from carbon fibers (PANEX 33 160K, ZOLTEK) wound into a titanium wire core (Logan et al. 2007), with a specific area based on the projected surface of 20 m^2/m^3 and a surface area based on individual fibers of 2,600 m^2/m^3. All anodes were heat treated for 30 min at 450 °C before use (Feng et al. 2010). The cathode contained a Pt catalyst layer (0.5 mg Pt/cm^2) on the solution side facing the anode. Reactors were equipped with an Ag/AgCl reference electrode (RE-5B, BASi) placed in the solution (15 mm far from the anode) in order to measure electrode potentials. Three anodes were placed in the main chamber, spaced 25-mm apart, and were connected externally by a single copper wire. The separators used in this study were either a glass fiber (Specialty Glass Products, NSG Co., Ltd.) or textile material (Amplitude Prozorb, Contec Inc.). The glass fiber separator was 1.2 mm thick with a weight of 150 g/m^2. The textile separator was made from 46% cellulose and 54% polyester (thickness = 0.3 mm; weight = 55 g/m^2). Two separator layers were placed between the anode and cathode to minimize oxygen crossover and possible short-circuiting between the electrodes.

MFC operation

The medium contained sodium acetate as the fuel (1.0 g/L) and a 50-mM phosphate buffer nutrient solution (PBS; conductivity of 6.82 mS/cm) containing Na$_2$HPO$_4$, 4.58 g/L; NaH$_2$PHO$_4$·H$_2$O, 2.45 g/L; NH$_4$Cl, 0.31 g/L; KCl, 0.13 g/L;

Fig. 1 Schematic design of MFC used in this study - (**a**) front view, (**b**) side view, and (**c**) photograph

(A)　　　　**(B)**　　　　**(C)**
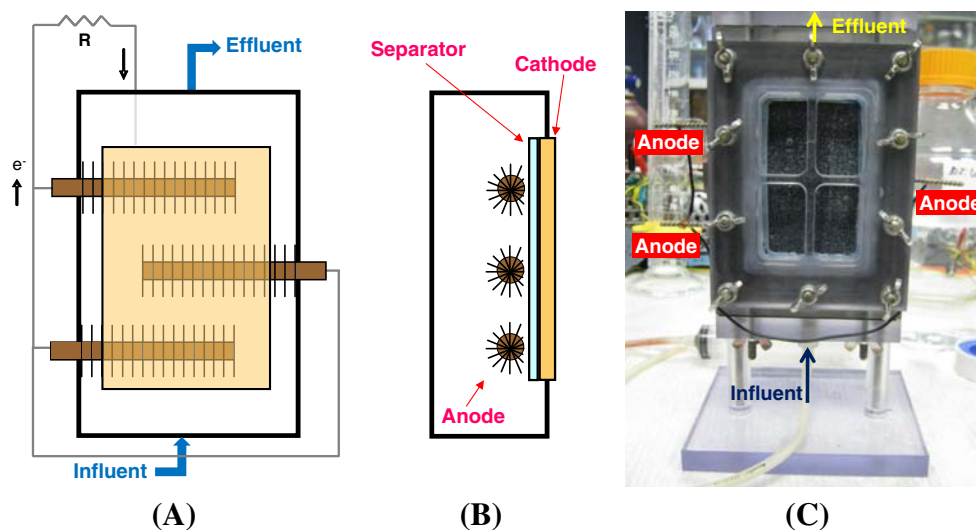
trace minerals (12.5 mL/L), and vitamins (5 mL/L) (Cheng et al. 2009). MFCs (duplicate reactors) were inoculated with domestic wastewater from the primary clarifier effluent at the Pennsylvania State University wastewater treatment plant. For the first two batch cycles, the reactor was filled with feed solutions containing 50% wastewater and 50% sodium acetate medium.

In fed-batch operation, reactors were refilled each time when the voltage decreased to less than 10 mV, forming one complete cycle of operation. MFCs were first acclimated to 1,000 Ω, and then the external resistance was switched to 200 Ω, and then to 50 Ω. MFCs ran for at least five fed-batch cycles at each resistance to ensure repeatable power output and steady conditions at each new resistance. Following fed-batch tests, continuous flow operation was initiated by feeding the medium to the bottom of the reactors at a rate of 390 mL/day (HRT, 8 h) with a peristaltic pump (Masterflex, Cole-Parmer, Vernon Hills, IL, USA). Additional HRTs were examined by setting the flow rates to 195 mL/day (HRT, 16 h) and 520 mL/day (HRT, 6 h). The organic loading rate was 1.9–5.1 g COD/L/day, which was similar to that in previous studies (0.1–4.8 g COD/L/day) (Moon et al. 2005; He et al. 2006; Aelterman et al. 2008; Zhang et al. 2008; Borole et al. 2011). All reactors were operated in a constant temperature room (30 °C).

Calculations and measurements

Cell voltages across the external resistor were measured every 40 min using a data acquisition system (Model 2700, Keithley Instrument) connected to a personal computer. Current, I (milliampere), was calculated according to $I = E/R_{ex}$, where E (millivolt) is the voltage and R_{ex} (ohm) is the external resistance. Power, P (milliwatt), was calculated according to $P = IV/1,000$. Current and power density were normalized by the cross-sectional area of the cathode.

In batch mode operation, polarization curves were obtained by the single-cycle method (20 min intervals) using multiple resistors as previously described (Watson and Logan 2011). For continuous operation mode, polarization curves were generated by varying the resistance from 1 to 40,000 Ω, with results at each resistor recorded after a stable voltage was achieved after a minimum of 4 h.

Chemical oxygen demand removal (ΔCOD) (percent) was calculated based on the initial and final measured COD. CE (percent) was calculated from COD removal, based on four electrons per mole of COD (Logan et al. 2006). COD was measured using standard methods [Method 5220, APHA 1995; high range (0–1,500 mg/L) HACH COD system (Hach Co., Loveland, CO, USA) (Cheng et al. 2006b; Jiang and Li 2009). The CE was calculated as: CE = $C_{out}/C_{in} \times 100\%$, where C_{out} is the total Coulombs actually transferred to the anode from the substrate, and C_{in} is the theoretical amount of Coulombs that can be produced from the substrate. The output charge was calculated by integrating the current over a certain time period (Δt), and the input charge was calculated as:

$$C_{in} = \frac{F \, b \, COD_{in} \, Q \, \Delta t}{M}$$

where F is the Faraday's constant, $b=4$ is the number of electrons exchanged per mole of oxygen, COD_{in} is the influent COD, Q is the flow rate, Δt is the time interval (the HRT) used to calculate output charge, and $M=32$ is the molecular weight of oxygen.

Internal resistance was characterized using electrochemical impedance spectroscopy (EIS). Scans were performed after the cell was run at an open-circuit condition for at least 5 h. The impedance measurements were taken from 100 kHz to 1 mHz by applying a sine wave (10 mV) on top of the

bias potentials with a potentiostat (BioLogic, VMP3). Anode and cathode charge transfer resistance was determined by fitting the EIS spectra with semi-circles (He and Mansfeld 2009; Hutchinson et al. 2011). The whole cell impedance value was determined from the projected point of intersection of the Nyquist plot and the *x*-axis (Hutchinson et al. 2011). To determine the charge transfer resistance, the data points of first circular section were fitted using software (EC-Lab V10.02, Bio-Logic SAS) to find a diameter of circle. Diffusion resistance was determined as the last point in the Nyquist plot.

Results

Enrichment

There was little current generation until day 9 (after three fed-batch cycles), when the maximum current was 0.17 mA, with the glass fiber separators (1,000 Ω) (Fig. 2). The CE was less than 1%, although most COD was removed (87±4%). The lack of power generation was unexpected given the high COD removal and results from previous smaller-scale tests (Zhang et al. 2009; Hays et al. 2011). Therefore, it was hypothesized that the electrodes were making contact through the glass fiber separator (short-circuiting). After replacing the glass fiber separator with the textile separators (day 25), the maximum current during a cycle increased to 0.65 mA, and the CE increased to 13±2% likely due to the reduced current with the lack of short-circuiting.

Reactor performance in fed-batch mode

All MFCs were acclimated to high external resistances (1,000 Ω), as it could shorten the lag phase for development
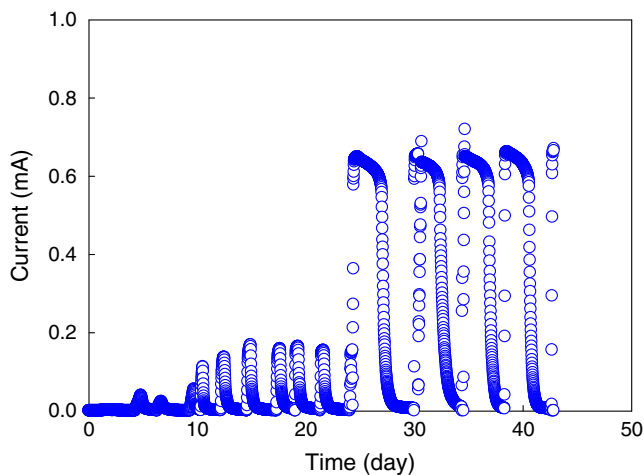
of an exoelectrogenic biofilm (Hong et al. 2011; Zhang et al. 2011a). The maximum voltage over a fed-batch cycle was 0.68 V at 1,000 Ω (Fig. 3), with each fed-batch cycle typically 3.8 days. When the MFCs were switched to a 200-Ω external resistance, the maximum current increased from 0.68 to 2.85 mA, while the maximum voltage slightly decreased to 0.57 V. When the external resistance was further reduced to 50 Ω, the maximum cell voltage decreased to 0.41 V. The highest maximum current of 8.24 mA was achieved at 20 Ω.

The polarization experiments were performed after running at least five batch cycles at single external resistance conditions. With MFCs acclimated to 50 Ω, the maximum power density was 975 mW/m^2 (30 W/m^3) based on polarization data. Power densities were 737 mW/m^2 (23 W/m^3), with MFCs acclimated to 200 Ω, and 467 mW/m^2 (14 W/m^3), when acclimated to 1,000 Ω (Fig. 4). The cathode potentials of the MFCs (Fig. 4) were similar when using the different external resistances, but the anode potentials changed. The anode potentials became more positive as the external resistance increased, likely due to increased oxygen intrusion into
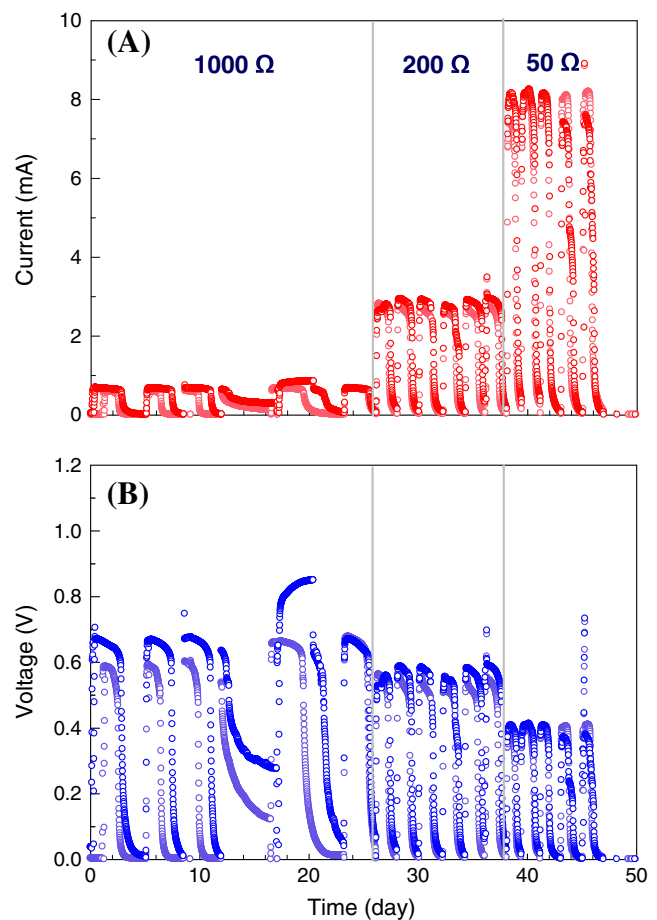

Fig. 2 Current production in a MFC during start-up with glass fiber (~25 days) or cleaning wipe (days 25~43) separators (50 mM PBS, 1,000 Ω resistor)

Fig. 3 Changes in (**a**) voltage and (**b**) current production for MFCs in batch mode operation with different external resistances (*different colors* represent data from duplicate reactors)
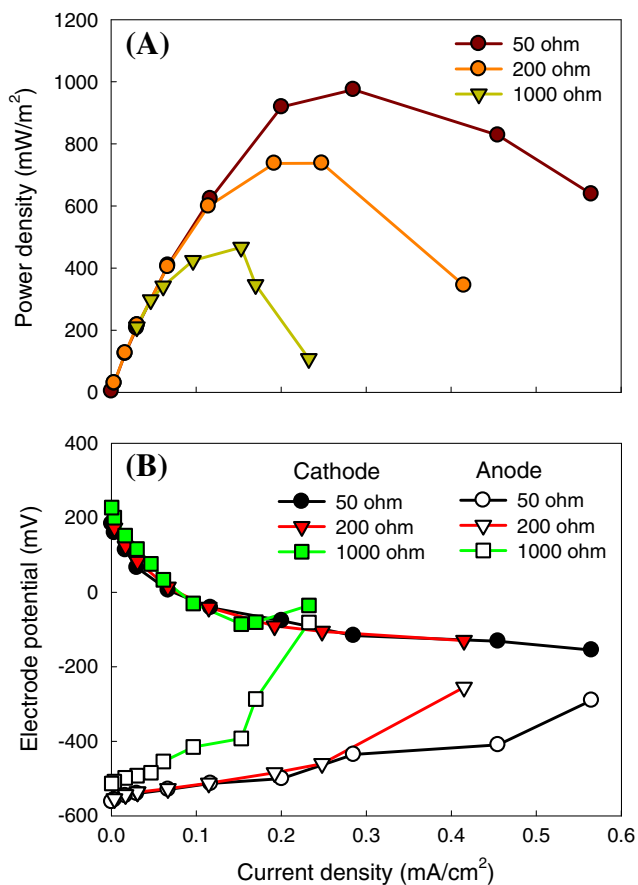
Fig. 4 (a) Power densities and (b) electrode potentials (vs. Ag/AgCl) as a function of current density for MFCs operated in fed-batch mode that were acclimated over several cycles to different external resistances
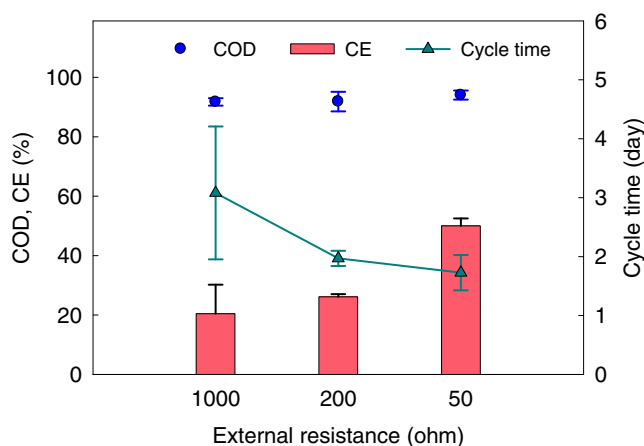

Fig. 5 COD removal, CE, and batch cycle time for MFCs with different external resistors

resistance to 50 Ω increased the current to 6.7 ± 0.5 mA, with an average voltage of 0.34 ± 0.03 V. This voltage was slightly lower than the maximum obtained in batch mode operation at this resistance (0.41 V at $R_{ext} = 50$ Ω). After switching to $R_{ext} = 10$ Ω, the current increased to 20 ± 2 mA with an average voltage of 0.28 ± 0.14 V.

the anode (Cheng et al. 2006a) as the length of a single batch cycle time increased.

COD removals were all over 90%. The highest CE of 53% was obtained with a 50-Ω resistor, with the lowest CE=20% at the highest resistance (Fig. 5). It was expected that the CE would increase with current densities due to less oxygen transfer into the reactor due to a shorter cycle time. For comparison, the CE of similar SEA configuration (28 mL) was increased from 35% to 71% by adding two layers of separator (J-cloth) (Fan et al. 2007). Smaller MFC tests (12 mL) with a similar SEA configuration achieved CEs ranging from 44% to 77% over a current density range of $0.8–4.0$ A/m² (Zhang et al. 2011b).

Continuous flow operation

The MFCs were operated under continuous flow conditions at three different HRTs (6, 8, and 16 h) (Fig. 6). During the first 10 days, the voltage fluctuated due to a poor electrical connection. After replacing the wires, a steady current of 2.6 ± 0.4 mA was obtained (200 Ω, 0.53 ± 0.08 V) with an HRT=8 h. A reduction in the external
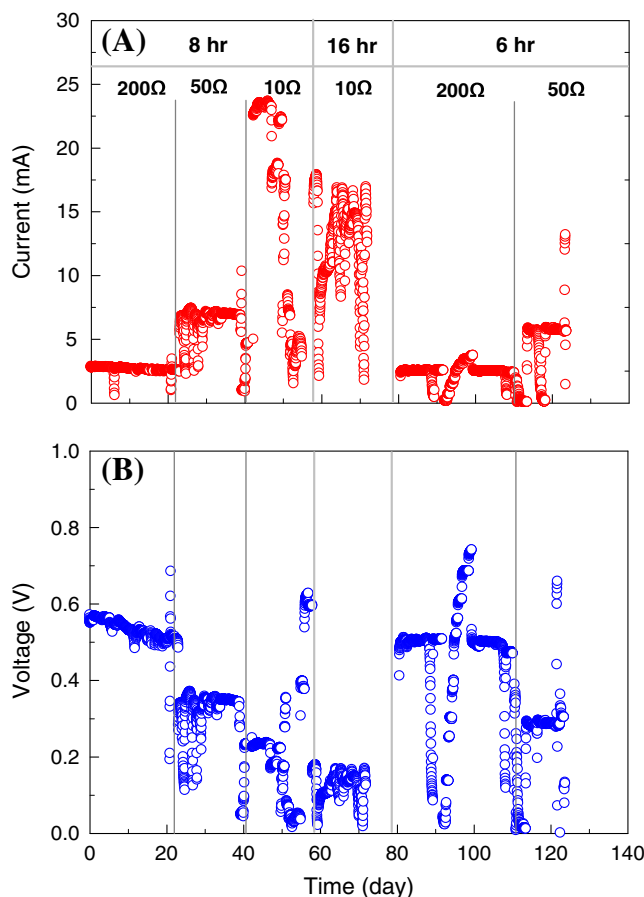

Fig. 6 (a) Cell voltage and (b) current production during continuous flow mode operation of MFCs (50 mM PBS)

After 58 days of operation, the HRT was increased to 16 h while maintaining an external resistance of 10 Ω. The current was reduced to 14 ± 3 mA and the voltage to 0.14 ± 0.03 V with a 10-Ω resistor. When the HRT was again decreased to 6 h (day 79), the average current output was 2.5 ± 0.3 mA, with an average voltage of 0.50 ± 0.02 V at $R_{ext}=200$ Ω. The current production was slightly less than that at an HRT=8 h (2.6 ± 0.4 mA). At a smaller external resistance of 50 Ω, the average current increased to 5.7 ± 0.1 mA (0.29 ± 0.01 V), which was also slightly lower than that with a longer HRT (6.7 ± 0.5 mA at HRT=8 h).

Polarization experiments were performed after the cell voltage stabilized at each set condition. The maximum power density was 880 mW/m^2 (24 W/m^3) with the MFCs operated at an HRT=8 h and an external resistance of 200 Ω (Fig. 7). The maximum power density slightly decreased to 865 mW/m^2 (23 W/m^3) at 50 Ω and to 834 mW/m^2 (23 W/m^3) at 10 Ω. With an HRT 16-h condition, the maximum power density was further reduced to 659 mW/m^2 (18 W/m^3), and type D power overshoot occurred (the power density curve doubles back at lower resistances).

COD removal was $52\pm14\%$ at an HRT=8 h ($R_{ext}=200$ Ω). At the lower resistances, the average COD removals were $52\pm9\%$ (50 Ω) and $55\pm6\%$ (10 Ω). These are lower COD removals than those obtained in fed-batch mode MFCs (>90%) due to the longer times allowed for a fed-batch cycle (Fig. 5). Increasing the HRT from 8 to 16 h increased COD removal from $55\pm6\%$ to $81\pm10\%$ at $R_{ext}=10$ Ω. With shorter HRT=6 h, the COD removals decreased to $37\pm8\%$ (200 Ω) and $35\pm6\%$ (50 Ω).

At an HRT of 8 h, the CE was $12\pm3\%$ ($R_{ext}=200$ Ω). Decreasing the resistance increased the CE to $32\pm13\%$ (50 Ω) and to $85\pm9\%$ (10 Ω). At a longer HRT=16 h, at the lowest resistance (10 Ω), the CE decreased to 80%, likely from increased oxygen intrusion into the reactor per amount of COD removed (Oh et al. 2009).
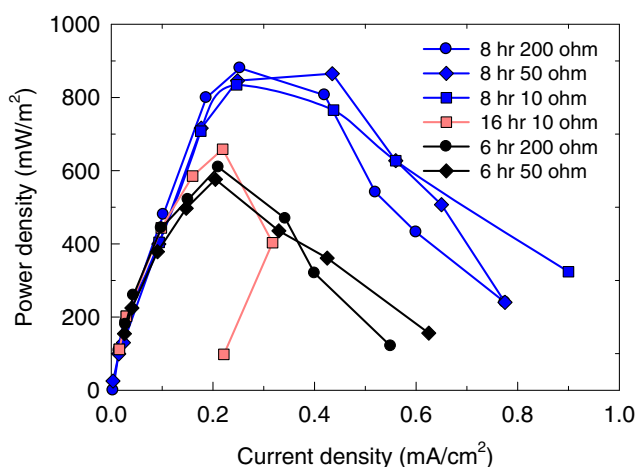
Internal resistance of MFCs

Identifying the factors that limit power production in an MFC system is critical for enhancing MFC performance. The total internal resistance was measured by two methods: from the linear portion of the polarization curve (Logan 2008) and through EIS analysis. Using polarization data, the internal resistance was calculated as 33 Ω (Fig. 8b). This was in good agreement with the sum of all resistances obtained using EIS of 33.8 Ω during continuous flow experiments (200 Ω) (Fig. 8a). Of the total internal resistance of 33 Ω (whole cell), the ohmic resistance was 2 Ω

Fig. 7 Power densities under different HRTs and external resistances for MFCs operated in continuous flow mode
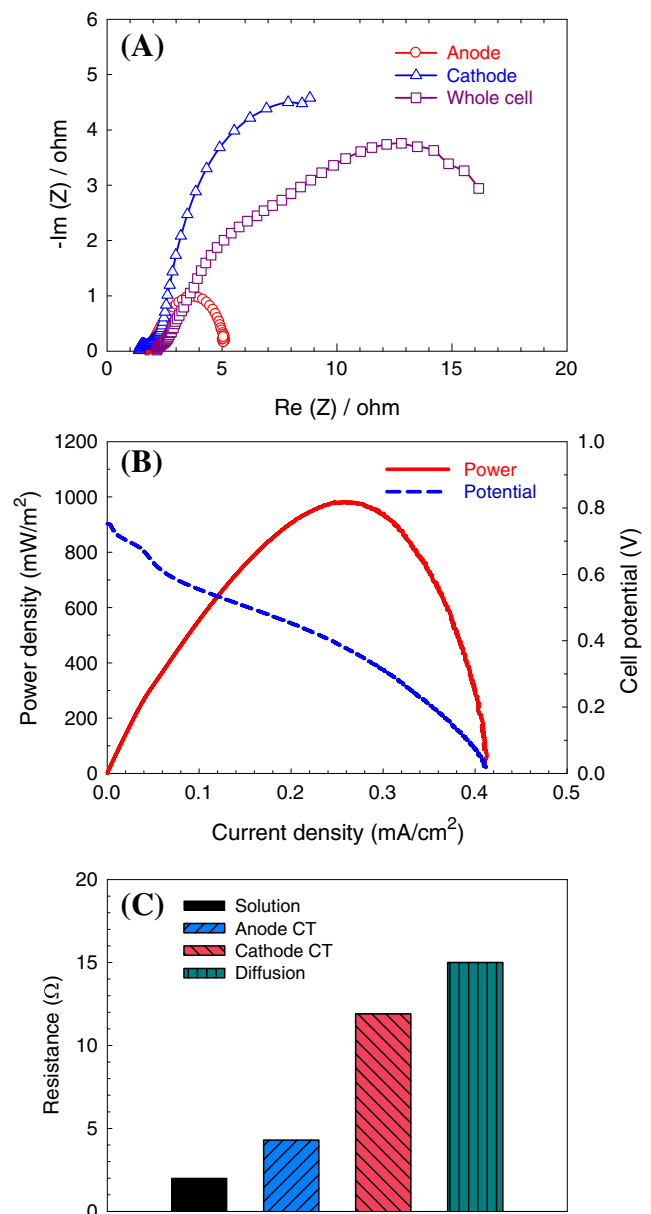

Fig. 8 (**a**) Nyquist plots of impedance spectra, (**b**) polarization curves, and (**c**) internal resistance distribution of continuous flow MFCs at an HRT=8 hr

(6.1%), the charge transfer resistance was 15 Ω (45.4%), and the diffusion resistance was 16 Ω (48.5%). The individual components of internal resistance were obtained from anode and cathode EIS data (Hutchinson et al. 2011). Cathode charge transfer resistance (11.9 Ω) was higher than the anode charge transfer resistance (4.3 Ω) (Fig. 8c).

Discussion

The performance of the larger-scale, SEA-type MFCs was generally comparable to that obtained in similar but smaller-scale systems. The maximum power density in fed-batch mode (986±20 mW/m^2) was only slightly less than that obtained from smaller reactors with brush to cathode spacing of 1.4 cm (940±100 mW/m^2) (Hutchinson et al. 2011). With a separator and closer-spaced electrodes using a similar SEA configuration and a glass fiber separator (Hays et al. 2011), the maximum power density in fed-batch mode was slightly larger (1,300 mW/m^2). It was recently found that the maximum power density is a linear function of the cathode-specific surface area (Cheng and Logan 2011). While the smaller reactors had a similar cathode-specific surface area (27 m^2/m^3, compared to 25 m^2/m^3 for the smaller reactor), the anode packing was smaller here, with a volume (milliliter) to number of brushes ratio of 43:1 (130 mL and three brushes) compared to 28:1 for the smaller reactor. The anode-specific area based on the individual fibers (2,600 m^2/m^3) was also lower than that of smaller MFCs (4,107 m^2/m^3). This suggests that the performance may have been affected by the lower brush packing density, even though there was a relatively large anode-specific surface area based on all brush fibers.

In fed-batch mode operation, we observed that the specific separator used was critical for increasing CE and power production. While glass fiber materials were shown to function well as separators in smaller reactors (Zhang et al. 2010a), a low CE (<1%) was obtained in this study, likely due to the deformation of the glass fibers that allowed the graphite fibers to penetrate the separator. Glass fiber separators have been found to have high proton and low oxygen transfer coefficients, but this material has a looser structure than other separators (Zhang et al. 2009). Thus, when large-pore separators were used, we found the material did not prevent electrical short-circuiting.

The CE can be increased with separators by reducing oxygen transfer to anode (Zhang et al. 2010b). For example, CE increased from 15–35% (no separator) to 18–76% (current density range of 0.7 to 4.8 A/m^2) by using nylon filter as separators in single-chamber air cathode MFCs (Zhang et al. 2010b). However, low CE (18–38%) was achieved with larger separator pores (160 μm) due to increased oxygen intrusion to the anode, and thus more substrate was lost to bacteria using oxygen. In fed-bath mode operation, CEs varied from 20% to 50% at current densities ranging from 0.2 to 2.3 A/m^2, which was

similar to that obtained in single-cathode MFCs at similar current densities (Zhang et al. 2011b). The CE value was largest (53%) for MFCs with a low resistor (50 Ω). Increased batch cycle time at high R_{ext} (Fig. 5) increased oxygen intrusion into the anode. Oxygen crossover in the reactor also affected power production. The cathode potential was almost similar for all external resistor conditions, but more negative anode potential was obtained in polarization tests (Fig. 4).

The average current output in continuous flow mode (6.7 mA, 50-Ω resistor) was slightly lower than the maximum value obtained in batch mode operation. The COD removal efficiency was also decreased in continuous flow mode (52–55%, HRT=8 h), likely due to a relatively shorter residence time compared to the much longer cycle time in fed-batch mode. In continuous flow mode, the COD removal could be increased by increasing the HRT, but this would also reduce overall power and current generation due to lower average substrate concentrations (Huang et al. 2009). The CE decreased slightly in continuous mode due to the increased oxygen intrusion. These results demonstrate that the HRT will need to be selected on the basis of either optimizing energy production or COD removal.

Internal resistances measured using either EIS or polarization curves were in good agreement. The total internal resistances measured here were higher than those reported for the smaller-scale SEA-type MFCs (11.8–12.2 Ω). However, the ohmic resistance here was only 2.2 Ω (6.1%), which was lower than that obtained for an upflow MFC (8.6 Ω) (He et al. 2005), a brush MFC even with a higher solution conductivity using 200 mM PBS (8 Ω) (Logan et al. 2007), and a double CEA MFC (3.9 Ω) (Fan et al. 2007). The reason for this lower ohmic resistance here is likely due to the close electrode spacing used in this SEA design.

It was demonstrated here that stable current and power can be produced using a multi-electrode continuous flow MFCs. Overall performance including maximum power density was comparable with small-scale MFCs. The performance of the continuous flow system was slightly less than that with fed-batch operation. The ohmic resistance here was much smaller than those of other MFCs. Thus, SEA-type multi-electrode MFCs could be used for treating low conductivity solutions, such as domestic wastewater.

References

Aelterman P, Rabaey K, Pham HT, Boon N, Verstraete W (2006) Continuous electricity generation at high voltages and currents using stacked microbial fuel cells. Environ Sci Technol 40 (10):3388–3394

Aelterman P, Versichele M, Marzorati M, Boon N, Verstraete W (2008) Loading rate and external resistance control the electricity generation of microbial fuel cells with different three-dimensional anodes. Bioresour Technol 99(18):8895–8902

APHA (1995) Standard methods for the examination of water and wastewater. American Public Health Association. 19th Edition. Washington, D.C.

Borole AP, Hamilton CY, Vishnivetskaya TA (2011) Enhancement in current density and energy conversion efficiency of 3-dimensional MFC anodes using pre-enriched consortium and continuous supply of electron donors. Bioresour Technol 102(8):5098–5104

Cheng SA, Logan BE (2007) Ammonia treatment of carbon cloth anodes to enhance power generation of microbial fuel cells. Electrochem Commun 9(3):492–496

Cheng SA, Logan BE (2011) Increasing power generation for scaling up single-chamber air cathode microbial fuel cells. Bioresour Technol 102(6):4468–4473

Cheng S, Liu H, Logan BE (2006a) Increased performance of single-chamber microbial fuel cells using an improved cathode structure. Electrochem Commun 8(3):489–494

Cheng S, Liu H, Logan BE (2006b) Increased power generation in a continuous flow MFC with advective flow through the porous anode and reduced electrode spacing. Environ Sci Technol 40 (7):2426–2432

Cheng SA, Xing DF, Call DF, Logan BE (2009) Direct biological conversion of electrical current into methane by electromethanogenesis. Environ Sci Technol 43(10):3953–3958

Cusick RD, Bryan B, Parker DS, Merrill MD, Mehanna M, Kiely PD, Liu G, Logan BE (2011) Performance of a pilot-scale continuous flow microbial electrolysis cell fed winery wastewater. Appl Microbiol Biotechnol 89(6):2053–2063

Dekker A, Ter Heijne A, Saakes M, Hamelers HVM, Buisman CJN (2009) Analysis and improvement of a scaled-up and stacked microbial fuel cell. Environ Sci Technol 43(23):9038–9042

Fan Y, Hu H, Liu H (2007) Enhanced coulombic efficiency and power density of air-cathode microbial fuel cells with an improved cell configuration. J Power Sources 171(2):348–354

Feng YJ, Yang Q, Wang X, Logan BE (2010) Treatment of carbon fiber brush anodes for improving power generation in air-cathode microbial fuel cells. J Power Sources 195(7):1841–1844

Hays S, Zhang F, Logan BE (2011) Performance of two different types of anodes in membrane electrode assembly microbial fuel cells for power generation from domestic wastewater. J Power Sources 196 (20):8293–8300

He Z, Mansfeld F (2009) Exploring the use of electrochemical impedance spectroscopy (EIS) in microbial fuel cell studies. Energy Environ Sci 2(2):215–219

He Z, Minteer SD, Angenent LT (2005) Electricity generation from artificial wastewater using an upflow microbial fuel cell. Environ Sci Technol 39(14):5262–5267

He Z, Wagner N, Minteer SD, Angenent LT (2006) An upflow microbial fuel cell with an interior cathode: assessment of the internal resistance by impedance spectroscopy. Environ Sci Technol 40 (17):5212–5217

Hong Y, Call DF, Werner CM, Logan BE (2011) Adaptation to high current using low external resistances eliminates power overshoot in microbial fuel cells. Biosens Bioelectron 28(1):71–76

Huang L, Cheng S, Rezaei F, Logan BE (2009) Reducing organic loads in wastewater effluents from paper recycling plants using microbial fuel cells. Environ Technol 30(5):499–504

Hutchinson AJ, Tokash JC, Logan BE (2011) Analysis of carbon fiber brush loading in anodes on startup and performance of microbial fuel cells. J Power Sources 196(22):9213–9219

Jiang D, Li B (2009) Granular activated carbon single-chamber microbial fuel cells (GAC-SCMFCs): a design suitable for large-scale wastewater treatment processes. Biochem Eng J 47(1–3):31–37

Liu H, Logan BE (2004) Electricity generation using an air-cathode single chamber microbial fuel cell in the presence and absence of a proton exchange membrane. Environ Sci Technol 38(14):4040–4046

Liu H, Cheng SA, Logan BE (2005a) Power generation in fed-batch microbial fuel cells as a function of ionic strength, temperature, and reactor configuration. Environ Sci Technol 39(14):5488–5493

Liu H, Cheng SA, Logan BE (2005b) Production of electricity from acetate or butyrate using a single-chamber microbial fuel cell. Environ Sci Technol 39(2):658–662

Liu H, Cheng S, Huang L, Logan BE (2008) Scale-up of membrane-free single-chamber microbial fuel cells. J Power Sources 179(1):274–279

Logan BE (2008) Microbial fuel cells. Wiley, Hoboken

Logan BE (2010) Scaling up microbial fuel cells and other bioelectrochemical systems. Appl Microbiol Biotechnol 85(6):1665–1671

Logan BE, Hamelers B, Rozendal R, Schröder U, Keller J, Freguia S, Aelterman P, Verstraete W, Rabaey K (2006) Microbial fuel cells: methodology and technology. Environ Sci Technol 40(17):5181–5192

Logan BE, Cheng S, Watson V, Estadt G (2007) Graphite fiber brush anodes for increased power production in air-cathode microbial fuel cells. Environ Sci Technol 41(9):3341–3346

Min B, Logan BE (2004) Continuous electricity generation from domestic wastewater and organic substrates in a flat plate microbial fuel cell. Environ Sci Technol 38(21):5809–5814

Moon H, Chang IS, Jang JK, Kim BH (2005) Residence time distribution in microbial fuel cell and its influence on COD removal with electricity generation. Biochem Eng J 27(1):59–65

Nevin KP, Richter H, Covalla SF, Johnson JP, Woodard TL, Orloff AL, Jia H, Zhang M, Lovley DR (2008) Power output and columbic efficiencies from biofilms of Geobacter sulfurreducens comparable to mixed community microbial fuel cells. Environ Microbiol 10(10):2505–2514

Oh SE, Kim JR, Joo JH, Logan BE (2009) Effects of applied voltages and dissolved oxygen on sustained power generation by microbial fuel cells. Water Sci Technol 60(5):1311–1317

Pham TH, Jang JK, Moon HS, Chang IS, Kim BH (2005) Improved performance of microbial fuel cell using membrane-electrode assembly. J Microbiol Biotechn 15(2):438–441

Rader GK, Logan BE (2010) Multi-electrode continuous flow microbial electrolysis cell for biogas production from acetate. Int J Hydrog Energ 35(17):8848–8854

Rozendal RA, Hamelers HVM, Molenkmp RJ, Buisman JN (2007) Performance of single chamber biocatalyzed electrolysis with different types of ion exchange membranes. Water Res 41(9):1984–1994

Watson VJ, Logan BE (2011) Analysis of polarization methods for elimination of power overshoot in microbial fuel cells. Electrochem Commun 13(1):54–56

Zhang JN, Zhao QL, You SJ, Jiang JQ, Ren NQ (2008) Continuous electricity production from leachate in a novel upflow air-cathode membrane-free microbial fuel cell. Water Sci Technol 57 (7):1017–1021

Zhang X, Cheng S, Wang X, Huang X, Logan BE (2009) Separator characteristics for increasing performance of microbial fuel cells. Environ Sci Technol 43(21):8456–8461

Zhang X, Cheng S, Huang X, Logan BE (2010a) Improved performance of single-chamber microbial fuel cells through control of membrane deformation. Biosens Bioelectron 25(7):1825–1828

Zhang X, Cheng S, Huang X, Logan BE (2010b) The use of nylon and glass fiber filter separators with different pore sizes in air-cathode single-chamber microbial fuel cells. Energy Environ Sci 3(5):659–664

Zhang L, Zhu X, Li J, Liao Q, Ye D (2011a) Biofilm formation and electricity generation of a microbial fuel cell started up under different external resistances. J Power Sources 196(15):6029–6035

Zhang X, Cheng S, Liang P, Huang X, Logan BE (2011b) Scalable air cathode microbial fuel cells using glass fiber separators, plastic mesh supporters, and graphite fiber brush anodes. Bioresour Technol 102(1):372–375